

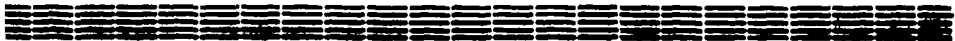
52

AT 9600012

YERPHI

Preprint YPI-1382(12)-92

ԵՐԵՎԱՆԻ ՖԻԶԻԿԱՅԻ ԻՆՍՏԻՏՈՒՏ
ЕРЕВАНСКИЙ ФИЗИЧЕСКИЙ ИНСТИТУТ
YEREVAN PHYSICS INSTITUTE



Ts. A. Amatuni, E. A. Mamidjanyan and Kh. N. Sanossyan

Monte-Carlo Simulation of Hadronic Shower
Part 2: The PION Calorimeter

ЦНИИатомниформ

Москва 1992

VOL 27 № 2 2

Յ. Ա ԱՄԱՏՈՒՆԻ, Է. Ա ՄԱԴԻՋԱՆՅԱՆ, Խ. Ն. ՍԱՆՈՍՅԱՆ

ՀԱԴԻՐՈՆԱՅԻՆ ՀԵՂԵՂՆԵՐԻ ԽԱՂԱՐԿՈՒՄԸ ՄՈՆՏԵ-ԶԱՐԼՈ ԵՂԱՆԱԿՈՎ

ՄԱՍ 2. «ՊԻՈՆ» ՏԵՂԱԿԱՅԱՆՔԻ ԿԱՆՈՐԻՄԵՏՐԸ

Էներգիայի արժեքի չորս միջակայքի համար, 0,5-ից մինչև 5ՏԷՎ տիրույթում, խաղարկված են հադրոնային հեղեղներ՝ օգտագործելով MARS 10 ծրագիրը եւ «ՊԻՈՆ» երկաթե իոնացման կալորիմետրի վրա ընկնող տիեզերական ճառագայթման հադրոնների էներգիական եւ անկյունային փորձարարական բաշխումները: Անջատված էներգիայի երկայնական բաշխումները համեմատված են փորձարարական տվյալների հետ՝ նկատվում է բավարար համանկումներ:

Հետազոտված են 0,3, 0,5, 1, 2, 5, 10 եւ 20ՏԷՎ էներգիաներով պրոտոնների, նեյտրոնների եւ պիոնների սկզբնավորած հադրոնային հեղեղների միջին բնութագրիչները: Գտնված են պարամետրացումներ հեղեղների երկայնական եւ լայնական պրոֆիլների համար: Առաջադրված է նոր ելակետային արտահայտություն լայնական պրոֆիլի համար: Գնահատված են արտահոսքը եւ ալբեդոն «ՊԻՈՆ» կալորիմետրից, ինչպես նաեւ արտահոսած եւ ալբեդո մասնիկների էներգիական բաշխումները:

ԵՐԵՎԱՆԻ ՖԻԶԻԿԱՅԻ ԻՆՍՏԻՏՈՒՏ

ԵՐԵՎԱՆ 1992



Центральный научно-исследовательский институт информации
и технико-экономических исследований по атомной науке
и технике (ЦНИИ Атоминформ) . 1992 г.

1. The Experimental Setup

The layout of the PION setup is given in fig.-s 2.1-2.3. It consists of a tracking part made up of six rows of multiwire proportional chambers(MWPC), a four module Transition Radiation Detector(TRD) to identify cosmic ray pions and protons, a removable 12cm thick carbon target and an iron ionization calorimeter (see ref. [1-4] for the details).

The setup is in operation since the late seventies and has been modernized several times since then. The fifth module of the TRD, the carbon target with 2 rows of MWPC (interaction detectors) and the scintillation detectors for EAS detection in the $10^{13} - 10^{15}$ eV energy range have been added. The setup is used for studies of the interaction of cosmic ray protons, pions and neutrons with C, Fe and Pb nuclei in the energy range of 500 - 10000GeV. In particular it was used for extensive measurements of pion/proton composition in cosmic radiation on Mt. Aragats (3250m above sea level) [5-7], inelastic cross sections for π -Fe, p-Fe and n-Fe interactions [8-11], neutron albedo from thick targets [12-16] and the distribution of the inelasticity partial coefficients of π -Fe, p-Fe and n-Fe interactions[17-20].

The ionization calorimeter consists of 10 layers of 10cm thick iron absorbers alternated by layers of 10cm in diameter cylindrical ionization chambers (IC) filled with argon mixture at 5atm. There are two additional layers of 3cm and 2cm thick lead absorbers on top of the calorimeter instrumented by similar layers of IC-s. The lateral dimension of the calorimeter is $3 \times 3 \text{m}^2$.

2. Comparison with Experiment

The experimental shower profiles were measured for hadrons in four energy intervals: 0.5-0.8TeV, 0.8-1.4TeV, 1.4-3TeV and 3-5TeV. The composition of the hadron flux was roughly 30%-pions and 70%-protons[21].

The Monte-Carlo simulations of the calorimeter were carried out with the help of the MARS10 code [22-24]. The simulations were performed in cylindrical geometry with the Z-axis pointed downwards and the origin at the middle of the upper surface of the first iron layer. The energy cutoff for Monte-Carlo was 4GeV. The number of simulated showers per each energy interval was 10000. The type, the energy and the azimuthal angle of the primary hadron are sampled from the experimental distributions corrected for the geometrical efficiency (see Tables 2.1 and 2.2).

Figure 4 shows the comparison between the average longitudinal profiles obtained in the experiment [21,25] and those from Monte-Carlo simulation. The Monte-Carlo and the experimental points are normalized at the shower maximum. As it can be seen from the figure, the agreement is satisfactory. Figure 5 shows the reduced lateral profiles for the same energy intervals obtained by simulations.

3. Shower Profiles in the PION Calorimeter

The longitudinal and lateral shower profiles were calculated for 0.3, 0.5, 1, 2, 5, 10 and 20TeV incident protons, neutrons and pions. The energy cutoff used in the Monte-Carlo simulations was 100MeV. For each energy value 5000 shower histories were run. The first interaction of the incident hadron was forced at $Z=0$.

The laterally integrated energy deposition of 5TeV proton induced showers in passive (Fe) and active (Ar) absorber layers is shown in fig. 2.6. Figure 2.7 shows the longitudinally integrated lateral profile (curve 1) and the lateral profile at the shower maximum (curve 2). It is seen, that the lateral profiles as a function of \sqrt{R} (the upper scale in fig. 2.7) clearly exhibit the two shower components - the sharply collimated hard core ($R < 1\text{cm}$) and the soft, wide shower tail ($R > 1\text{cm}$).

Proton, neutron and pion induced longitudinal shower profiles for 0.3, 0.5, 1, 2, 5, 10 and 20TeV are presented in fig.-s 2.8 a), b) and

c) respectively. One can see, that within the statistical errors, proton, neutron and pion induced shower profiles do not differ significantly.

The longitudinally integrated lateral profiles for proton, neutron and pion induced showers normalized to the incident energy values are given in fig. 2.9 a), b) and c) respectively. The reduced lateral profiles weakly depend on the primary energy. A weak tendency of narrowing of the shower core with the increase of the primary energy can be seen from fig. 2.9 and Table 2.3. The fraction of primary energy deposited in a circle of radius $R < 1\text{cm}$ slowly increases with the primary energy while for $R > 1\text{cm}$ it slowly decreases.

The reduced lateral shower profiles for proton, neutron and pion induced showers at the shower maximum are presented in Table 2.4. The reduced lateral profiles for the same showers in the first and sixth layers of the PION calorimeter are given in Tables 2.5 and 2.6 respectively.

4. Parametrization of the Longitudinal and Lateral Shower Profiles

The longitudinal shower profiles were parametrized by the following function [26,27]:

$$dE/dx = N_L [W_L (x/X_0)^{a-1} e^{-b(x/X_0)} + (1-W_L)(x/\lambda)^{c-1} e^{-d(x/\lambda)}], \quad (2.1)$$

where

x/X_0 - is the depth from the shower origin in radiation lengths,

x/λ - is the depth from the shower origin in absorption lengths,

W_L - is the relative weight of the two components,

a, b, c, d - are shape parameters which along with W_L are obtained from a fit,

N_L - is fixed by the normalization condition

$$\int_0^\infty (dE/dx) dx = E_0, \quad (2.2)$$

giving

$$N_L = E_0 [W_L X_0 \Gamma(a)/b^a + (1 - W_L) \lambda \Gamma(c)/d^c], \quad (2.3)$$

where

$$\Gamma(p) = \int_0^{\infty} t^{p-1} e^{-t} dt \quad (2.4)$$

is the Gamma function [28].

The five parameters a , b , c , d and W_L were obtained from a χ^2 - fit to the Monte-Carlo points with

$$\chi^2 = \sum [(1/E_0)(\Delta E/\Delta x) - (1/\Delta x) \int_{x_0}^{x_0+\Delta x} (1/E_0)(dE/dx)]^2 / \sigma^2. \quad (2.5)$$

The χ^2 minimization was performed by MINUIT [29].

The energy dependence of the fitted values of a , b , c , d and W_L are given in fig. 2.10. As it can be seen from the figures a , b , c and d are slowly (logarithmically) increasing functions of the primary energy. Within the statistical errors they do not depend on the type of the primary (proton, neutron or pion). The shape parameters of the longitudinal profiles were in their turn fitted to the straight lines in log scale for a , b , c , d and in log-log scale for W_L . The simple expressions for them are listed in Table 2.7. Figure 2.11 shows the energy dependence of the shower maximum depth. It was parametrized by the form

$$X_{max} = \tau \lg E_0, \quad E_0 \text{ in GeV}, \quad (2.6)$$

and the values of the coefficient for various primaries are listed in Table 2.8.

The fraction of shower energy deposited in the form of electromagnetic cascades due to neutral pions, as a function of primary energy is given in fig. 2.12. It can be seen, that the fraction of electromagnetic energy increases with incident energy constituting almost 80% at 10 TeV.

The lateral shower profiles were fitted by the form

$$f(R) = N_T [W_T (\rho_1/2) e^{-\rho_1 R} + (1 - W_T) (\rho_2/2) e^{-\rho_2 R}], \quad (2.7)$$

where

- R - is the distance from the shower axis,
- N_T - is a normalization coefficient,
- W_T - represents the weight of the two components and
- D_1, D_2 - are shape parameters. The values of N_T, W_T, D_1 and D_2 were obtained from a least squares fit

$$\chi^2 = \Sigma[(1/E_0)(\Delta E/\Delta R) - (1/\Delta R) \int_0^{\Delta R} r(R) dR]^2 / \sigma^2 \quad (2.8)$$

for the Monte-Carlo data from Table 2.3. The energy dependence of the parameter values are given in fig.-s 2.13, 2.14 and 2.15 for proton, neutron and pion initiated showers respectively. A sample of simulated lateral profiles and fits with the expression (2.7) are given in fig. 2.16. The lateral shower profiles at the shower maximum (see Table 2.4) were also fitted with the expression (2.7). The values of the coefficients for various primary particle types and energies are given in Table 2.9. It is seen from fig. 2.16 and Table 2.9 that expression (2.7) describes the lateral shower profiles quite well.

5. Leakage and albedo from the PION Calorimeter

The leakage energy and the number of leakage particles for 0.3, 0.5, 1, 2, 5, 10 and 20TeV proton, neutron and pion induced showers in the PION calorimeter are presented in Tables 2.10, 2.11 and 2.12. The energy dependence of the energy leakage from the calorimeter for proton, neutron and pion induced showers is given in fig. 2.17. Figure 2.18 shows the average number of particles escaping the calorimeter bottom surface as function of incident energy. The average energy carried off by albedo particles is presented in fig. 2.19. The energy dependence of the average number of albedo particles is given in fig. 2.20. The energy dependence of the total (forward + side + albedo) leakage energy for proton, neutron and pion induced showers is given in fig. 2.21. Figure 2.22 shows the energy dependence of the total number of leakage particles. The average

energy carried off by one leakage particle as a function of incident energy is presented in fig. 2.23.

The energy spectrum of leakage particles (protons, neutrons and charged pions) from the bottom surface of the calorimeter for 1, 2 and 20TeV proton induced showers are presented in fig. 2.24. The energy spectrum of albedo neutrons for the same cascades are presented in fig. 2.25.

ACKNOWLEDGEMENTS

We thank Dr. V. Avakyan for his continuous interest in this work and Dr. N. Mokhov who kindly made available MARS10 code for us.

TABLES

Table 2-1. Experimentally measured energy distribution of cosmic ray hadrons at 3250m altitude [25,21].

$\Delta E, \text{ GeV}$	$\langle E \rangle = \sum E_i N_i / \sum N_i$	ΔN_i	$\langle S \Omega \rangle_{\text{tot}} = 0.43753$	Cumulative
500-600		336	767.95	0.3858
600-700	639	290	662.81	0.7187
700-800		245	559.96	1.
800-1000		356	813.66	0.5122
1000-1200	1036	206	470.82	0.8086
1200-1400		133	303.98	1.
1400-1600		87	198.84	0.2949
1600-2000	1955	104	237.7	0.6475
2000-3000		104	237.7	1.
3000-4000		35	79.99	0.814
4000-5000	3690	8	18.28	1.
> 5000		11	25.14	

Table 2-2. Experimentally measured azimuthal angle($\cos\theta$) distribution of cosmic ray hadrons [25,21].

$$\Delta = (\cos 0^\circ - \cos 30^\circ) / 10 \approx 0.0134$$

$\cos\theta$	$\Delta = 0.0134$	$2\Delta = 0.0268$	$3\Delta = 0.0402$	$4\Delta = 0.0536$								
Interval	0.9866-1.0	0.9598-0.9866	0.9196-0.9598	0.866-0.9196								
$\Delta E_0, \text{GeV}$	N_i	Cumul.	N_i	Cumul.	N_i	Cumul.	N_i	Cumul.				
500- 800	208	334.9	1	278	525.2	0.8104	225	520.3	0.5131	135	386.2	0.2186
800-1400	171	275.3	1	221	417.5	0.6958	164	379.7	0.4952	105	300.3	0.2188
1400-3000	69	111.1	1	91	171.9	0.8068	78	180.4	0.5078	39	111.6	0.1941
3000-5000	10	16.1	1	10	18.9	0.6102	14	32.4	0.3826	7	20.0	0.1211

Table 2-3. Reduced longitudinally integrated lateral energy deposition for p, n, π^- induced showers.
 $(10^3/E_0)(\Delta E_{\text{total}}/\Delta R)$.

a) Proton induced showers.

E_0 , GeV	300	500	1000	2000	5000	10000	20000
R, cm							
1	230.0 ± 4.0	264.0 ± 4.0	299.0 ± 5.0	338.0 ± 5.0	372.0 ± 7.0	395.0 ± 6.0	421.0 ± 7.0
2	124.0 ± 3.0	125.0 ± 3.0	126.0 ± 3.0	124.0 ± 5.0	122.0 ± 3.0	114.0 ± 3.0	123.0 ± 3.0
4	65.0 ± 1.0	67.0 ± 1.0	65.0 ± 2.0	63.0 ± 1.0	58.0 ± 2.0	54.0 ± 1.0	54.0 ± 1.0
6	38.0 ± 1.0	36.0 ± 0.2	34.0 ± 1.0	32.0 ± 1.0	28.0 ± 1.0	26.0 ± 1.0	27.0 ± 1.0
8	24.0 ± 1.0	23.0 ± 0.7	21.0 ± 1.0	20.0 ± 1.0	17.0 ± 1.0	16.0 ± 1.0	16.0 ± 1.0
10	18.0 ± 1.0	15.9 ± 0.6	15.0 ± 1.0	14.0 ± 1.0	12.0 ± 1.0	11.0 ± 1.0	11.0 ± 0.001
20	8.3 ± 0.3	7.4 ± 0.2	6.8 ± 0.2	6.5 ± 0.3	5.2 ± 0.2	4.7 ± 0.2	4.4 ± 0.1
40	1.9 ± 0.1	1.55 ± 0.03	1.6 ± 0.1	1.3 ± 0.1	1.0 ± 0.1	0.9 ± 0.1	0.75 ± 0.04
80	0.2 ± 0.01	0.18 ± 0.01	0.19 ± 0.02	0.16 ± 0.03	0.12 ± 0.01	0.083 ± 0.008	0.086 ± 0.008
150	0.016 ± 0.004	0.019 ± 0.003	0.018 ± 0.003	0.015 ± 0.003	0.014 ± 0.004	0.007 ± 0.002	0.006 ± 0.001

2-3. b) Neutron induced showers.

E_0 , GeV	300	500	1000	2000	5000	10000	20000
R, cm							
1	226.0 ± 4.0	256.0 ± 5.0	298.0 ± 5.0	331.0 ± 5.0	384.0 ± 6.0	393.0 ± 6.0	400.0 ± 6.0
2	120.0 ± 3.0	124.0 ± 3.0	127.0 ± 3.0	124.0 ± 3.0	123.0 ± 3.0	121.0 ± 3.0	114.0 ± 3.0
4	69.0 ± 3.0	68.0 ± 2.0	63.0 ± 2.0	58.0 ± 1.0	58.0 ± 2.0	51.0 ± 1.0	51.0 ± 1.0
6	40.0 ± 2.0	34.0 ± 1.0	33.0 ± 1.0	31.0 ± 1.0	28.0 ± 1.0	29.0 ± 1.0	25.0 ± 1.0
8	25.0 ± 1.0	23.0 ± 1.0	22.0 ± 1.0	19.0 ± 1.0	18.0 ± 1.0	16.0 ± 1.0	15.0 ± 1.0
10	16.0 ± 1.0	15.0 ± 1.0	15.0 ± 1.0	14.0 ± 1.0	13.0 ± 0.5	10.0 ± 0.5	9.8 ± 0.5
20	8.3 ± 0.2	7.5 ± 0.2	6.5 ± 0.2	6.1 ± 0.2	5.0 ± 0.1	4.4 ± 0.2	3.9 ± 0.1
40	1.9 ± 0.1	1.6 ± 0.1	1.5 ± 0.1	1.4 ± 0.1	1.0 ± 0.05	0.89 ± 0.06	0.74 ± 0.04
80	0.22 ± 0.0	0.23 ± 0.02	0.17 ± 0.01	0.15 ± 0.01	0.11 ± 0.01	0.09 ± 0.01	0.082 ± 0.007
150	0.016 ± 0.002	0.014 ± 0.002	0.015 ± 0.002	0.024 ± 0.015	0.011 ± 0.002	0.01 ± 0.002	0.011 ± 0.003

2-3. c) Pion induced showers.

E_0 , GeV	300	500	1000	2000	5000	10000	20000
R , cm							
1	266.0 ± 6.0	286.0 ± 6.0	331.0 ± 6.0	326.0 ± 7.0	368.0 ± 7.0	377.0 ± 7.0	398.0 ± 8.0
2	109.0 ± 3.0	112.0 ± 3.0	111.0 ± 3.0	113.0 ± 4.0	111.0 ± 4.0	108.0 ± 4.0	108.0 ± 4.0
4	55.0 ± 2.0	62.0 ± 1.0	58.0 ± 3.0	49.0 ± 2.0	49.0 ± 2.0	45.0 ± 2.0	47.0 ± 2.0
6	36.0 ± 1.0	33.0 ± 1.0	32.6 ± 2.0	25.0 ± 1.0	24.0 ± 1.0	22.0 ± 1.0	20.0 ± 1.0
8	20.0 ± 1.0	21.0 ± 1.0	18.0 ± 1.0	16.0 ± 1.0	14.0 ± 1.0	15.0 ± 1.0	13.0 ± 1.0
10	14.0 ± 1.0	14.0 ± 1.0	14.0 ± 1.0	9.1 ± 5.0	8.8 ± 6.5	9.2 ± 6.6	8.5 ± 6.7
20	6.5 ± 0.7	7.9 ± 0.5	6.6 ± 0.3	4.5 ± 0.2	4.1 ± 0.2	3.4 ± 0.2	3.3 ± 0.2
40	1.4 ± 0.1	1.9 ± 0.3	1.6 ± 0.1	0.88 ± 0.04	0.77 ± 0.04	0.68 ± 0.05	0.75 ± 0.06
80	0.18 ± 0.02	0.29 ± 0.08	0.22 ± 0.03	0.10 ± 0.01	0.09 ± 0.01	0.081 ± 0.01	0.078 ± 0.01
150	0.01 ± 0.001	0.059 ± 0.021	0.022 ± 0.004	0.006 ± 0.001	0.009 ± 0.004	0.01 ± 0.002	0.006 ± 0.002

Table 2-4. Reduced lateral energy deposition for p, n, π^- induced showers at the shower maximum.
 $(10^3/E_0)(\Delta E_{\text{max}}/\Delta R)$ at maximum of the longitudinal shower profile.
 $(E_{\text{cut}}=100\text{MeV}, N=5000, \text{ the 1-st interaction is forced on Fe1}).$

a) Proton induced showers.

$E_0, \text{ GeV}$	300	500	1000	2000	5000	10000	20000
1	184.0 ± 2.0	197.0 ± 3.0	107.0 ± 3.0	112.0 ± 3.0	190.0 ± 4.0	101.0 ± 3.0	106.0 ± 3.0
2	139.0 ± 2.0	138.0 ± 2.0	32.0 ± 1.0	25.0 ± 1.0	133.0 ± 2.0	28.0 ± 1.0	28.0 ± 1.0
4	117.0 ± 1.0	116.0 ± 1.0	12.0 ± 1.0	11.0 ± 0.6	114.0 ± 0.8	12.0 ± 1.0	11.0 ± 1.0
6	8.1 ± 0.4	7.1 ± 0.4	4.6 ± 0.3	3.4 ± 0.3	5.3 ± 0.4	5.1 ± 0.4	4.7 ± 0.4
8	4.7 ± 0.3	3.9 ± 0.3	2.7 ± 0.2	2.2 ± 0.2	3.2 ± 0.3	2.9 ± 0.3	2.8 ± 0.3
10	2.9 ± 0.2	2.5 ± 0.3	1.4 ± 0.14	1.3 ± 0.2	2.0 ± 0.3	1.8 ± 0.2	1.5 ± 0.2
20	1.1 ± 0.1	0.93 ± 0.05	0.67 ± 0.05	0.54 ± 0.04	0.74 ± 0.08	0.72 ± 0.06	0.51 ± 0.05
40	0.16 ± 0.02	0.13 ± 0.01	0.13 ± 0.01	0.075 ± 0.009	0.13 ± 0.02	0.01 ± 0.014	0.078 ± 0.01
80	0.017 ± 0.004	0.009 ± 0.001	0.01 ± 0.003	0.019 ± 0.005	0.014 ± 0.004	0.004 ± 0.001	0.011 ± 0.004
150	0.003 ± 0.0014	0.0015 ± 0.0006	0.002 ± 0.001	0.0004 ± 0.0001	0.0018 ± 0.0009	0.0013 ± 0.0009	0.0002 ± 0.0001

2-4. b) Neutron induced showers.

E_0 , GeV	300	500	1000	2000	5000	10000	20000
R , cm							
1	88.0 ±3.0	92.0 ±3.0	105.0 ±3.0	111.0 ±3.0	91.0 ±3.0	99.0 ±3.0	108.0 ± 3.0
2	42.0 ±2.0	36.0 ±1.0	31.0 ±1.0	28.0 ±1.0	32.0 ±1.0	30.0 ±1.0	28.0 ± 1.0
4	17.0 ±1.0	17.0 ±1.0	12.0 ±1.0	10.0 ±1.0	13.0 ±1.0	12.0 ±0.67	11.0 ± 1.0
6	8.3 ±0.4	6.6 ±0.4	5.2 ±0.3	4.1 ±0.3	5.1 ±0.4	5.4 ±0.4	4.6 ± 0.4
8	5.3 ±0.3	3.9 ±0.3	3.0 ±0.2	2.0 ±0.2	2.7 ±0.2	2.6 ±0.3	2.6 ± 0.3
10	3.1 ±0.3	2.4 ±0.2	1.8 ±0.2	1.3 ±0.2	2.2 ±0.2	1.6 ±0.2	1.4 ± 0.2
20	1.2 ±0.1	0.96 ±0.06	6.9 ±0.05	0.51 ±0.04	0.78 ±0.06	0.53 ±0.05	0.45 ± 0.05
40	0.19 ±0.02	0.17 ±0.02	0.09 ±0.01	0.073 ±0.01	0.11 ±0.02	0.096 ±0.01	0.072 ± 0.01
80	0.02 ±0.005	0.014 ±0.002	0.011 ±0.003	0.010 ±0.003	0.015 ±0.004	0.013 ±0.004	0.008 ± 0.002
150	0.0012 ±0.0004	0.0014 ±0.0005	0.0015 ±0.0009	0.0003 ±0.0001	0.0017 ±0.0008	0.0008 ±0.0006	0.0

2-4. c) Pion induced showers.

E_0 , GeV	300	500	1000	2000	5000	10000	20000
R, cm							
1.	110.0 ± 4.0	119.0 ± 4.0	128.0 ± 4.0	84.0 ± 3.0	105.0 ± 4.0	108.0 ± 4.0	112.0 ± 4.0
2.	34.0 ± 1.0	32.0 ± 2.0	27.0 ± 1.0	33.0 ± 2.0	31.0 ± 2.0	28.0 ± 2.0	26.0 ± 1.0
4.	14.0 ± 1.0	13.0 ± 1.0	9.4 ± 0.6	14.0 ± 1.0	12.0 ± 1.0	11.0 ± 1.0	10.0 ± 1.0
6.	5.4 ± 0.3	5.0 ± 0.4	4.9 ± 0.4	5.6 ± 0.4	5.7 ± 0.5	4.7 ± 0.5	4.3 ± 0.4
8.	3.2 ± 0.2	2.8 ± 0.2	2.9 ± 0.1	3.5 ± 0.3	3.1 ± 0.4	2.5 ± 0.3	2.5 ± 0.4
10.	2.2 ± 0.2	1.8 ± 0.2	2.1 ± 0.4	2.1 ± 0.3	2.0 ± 0.2	1.6 ± 0.2	1.4 ± 0.2
20.	0.93 ± 0.08	0.88 ± 0.08	0.54 ± 0.05	0.78 ± 0.06	0.68 ± 0.07	0.54 ± 0.06	0.43 ± 0.06
40.	0.13 ± 0.01	0.13 ± 0.02	0.09 ± 0.012	0.1 ± 0.01	0.086 ± 0.014	0.078 ± 0.012	0.053 ± 0.012
80.	0.011 ± 0.003	0.018 ± 0.004	0.009 ± 0.002	0.009 ± 0.003	0.010 ± 0.003	0.014 ± 0.008	0.011 ± 0.004
150.	0.0008 ± 0.0006	0.003 ± 0.002	0.002 ± 0.001	0.001 ± 0.0005	0.0008 ± 0.0005	0.0005 ± 0.0003	0.0007 ± 0.0004

Table 2-5. Reduced lateral energy deposition of p, n, π^- induced showers at the first iron row.
 $(10^3/E_0)(\Delta E_{Fe1}/\Delta R)$ at 10cm depth of Fe/Ar sandwich.
 $(E_{cut}=100\text{MeV}, N=5000, \text{the 1-st interaction is forced on Fe1}).$

a) Proton induced showers.

$E_0, \text{ GeV}$	300	500	1000	2000	5000	10000	20000
$R, \text{ cm}$							
1.	68.0 ±2.0	58.0 ±2.0	46.0 ±2.0	36.0 ±1.0	24.0 ± 1.0	18.0 ± 1.0	11.0 ±1.0
2.	14.0 ±1.0	10.0 ±1.0	6.1 ±0.4	3.8 ±0.3	2.4 ± 0.3	1.4 ± 0.16	0.67 ±0.1
4.	5.0 ±0.2	3.5 ±0.2	0.2 ±0.01	1.5 ±0.1	0.8 ± 0.1	0.49 ± 0.05	0.31 ±0.05
6.	1.9 ±0.1	1.5 ±0.1	0.1 ±0.01	0.66 ±0.1	0.28 ± 0.03	0.2 ± 0.04	0.096 ±0.01
8.	1.2 ±0.1	0.75 ±0.06	0.051 ±0.008	0.36 ±0.06	0.2 ± 0.03	0.11 ± 0.02	0.051 ±0.01
10.	0.65 ±0.07	0.4 ±0.05	0.035 ±0.005	0.14 ±0.02	0.25 ± 0.07	0.094 ± 0.03	0.033 ±0.007
20.	0.17 ±0.01	0.11 ±0.01	0.012 ±0.002	0.043 ±0.005	0.03 ± 0.005	0.024 ± 0.006	0.019 ±0.005
40.	0.026 ±0.006	0.027 ±0.008	0.015 ±0.004	0.022 ±0.007	0.003 ± 0.0007	0.003 ± 0.001	0.0019 ±0.0007
80.	0.0033 ±0.0007	0.0027 ±0.001	0.007 ±0.0042	0.003 ±0.002	0.002 ± 0.001	0.0005 ±0.0002	0.0009 ±0.0005
150.	0.0004 ±0.0002	0.0005 ±0.0001	0.0001 ±0.00001	0.0001 ±0.00001	0.0	0.0	0.0

2-5. b) Neutron induced showers.

E_0 , GeV	300	500	1000	2000	5000	10000	20000
R, cm							
1.	69.0 ± 2.0	58.0 ± 2.0	49.0 ± 2.0	37.0 ± 1.0	27.0 ± 1.0	18.0 ± 1.0	13.0 ± 1.0
2.	12.4 ± 0.5	9.2 ± 0.5	6.4 ± 0.4	4.9 ± 0.4	2.1 ± 0.2	1.3 ± 0.1	0.62 ± 0.07
4.	4.8 ± 0.2	3.5 ± 0.2	2.3 ± 0.2	1.4 ± 0.1	0.9 ± 0.1	0.5 ± 0.1	0.35 ± 0.08
6.	2.3 ± 0.2	1.5 ± 0.1	0.87 ± 0.07	0.54 ± 0.05	0.34 ± 0.06	0.23 ± 0.6	0.12 ± 0.02
8.	1.0 ± 0.1	0.67 ± 0.05	0.39 ± 0.003	0.32 ± 0.05	0.21 ± 0.04	0.13 ± 0.03	0.23 ± 0.2
10.	0.56 ± 0.06	0.38 ± 0.04	0.27 ± 0.03	0.21 ± 0.05	0.12 ± 0.03	0.049 ± 0.008	0.032 ± 0.005
20.	0.18 ± 0.02	0.13 ± 0.01	0.085 ± 0.01	0.061 ± 0.01	0.046 ± 0.01	0.06 ± 0.02	0.014 ± 0.003
40.	0.026 ± 0.006	0.026 ± 0.008	0.016 ± 0.005	0.014 ± 0.005	0.0032 ± 0.001	0.02 ± 0.01	0.008 ± 0.005
80.	0.008 ± 0.004	0.0038 ± 0.001	0.0022 ± 0.0008	0.0017 ± 0.0009	0.0008 ± 0.0005	0.0007 ± 0.0003	0.0009 ± 0.0006
150.	0.0001 ± 0.00001	0.0007 ± 0.0005	0.0	0.0	0.0	0.0	0.0

2-5. c) Pion induced showers.

E_0 , GeV	300	500	1000	2000	5000	10000	20000
1.	61.0 ± 2.0	51.0 ± 2.0	41.0 ± 2.0	29.0 ± 1.0	17.0 ± 1.0	13.0 ± 1.0	9.0 ± 0.7
2.	8.5 ± 4.4	7.0 ± 0.5	3.8 ± 0.3	2.4 ± 0.2	1.5 ± 0.2	0.9 ± 0.1	0.57 ± 0.12
4.	3.6 ± 0.2	2.5 ± 0.2	1.6 ± 0.1	1.0 ± 0.1	0.53 ± 0.08	0.37 ± 0.08	0.13 ± 0.01
6.	1.5 ± 0.1	1.1 ± 0.1	0.58 ± 0.05	0.33 ± 0.04	0.2 ± 0.02	0.13 ± 0.02	0.076 ± 0.01
8.	0.61 ± 0.05	0.8 ± 0.1	0.3 ± 0.03	0.21 ± 0.04	0.1 ± 0.02	0.046 ± 0.007	0.063 ± 0.03
10.	0.32 ± 0.03	0.4 ± 0.08	0.23 ± 0.06	0.11 ± 0.03	0.086 ± 0.03	0.023 ± 0.003	0.015 ± 0.002
20.	0.13 ± 0.02	0.098 ± 0.009	0.061 ± 0.008	0.04 ± 0.008	0.026 ± 0.008	0.0068 ± 0.0008	0.006 ± 0.0008
40.	0.014 ± 0.003	0.01 ± 0.004	0.0093 ± 0.003	0.005 ± 0.002	0.0028 ± 0.0009	0.0041 ± 0.002	0.002 ± 0.0005
80.	0.0036 ± 0.002	0.007 ± 0.003	0.0029 ± 0.002	0.002 ± 0.001	0.0035 ± 0.003	0.0002 ± 0.00006	0.0001 ± 0.00005
150.	0.0002 ± 0.0001	0.0009 ± 0.0004	0.0005 ± 0.0004	0.0003 ± 0.0002	0.0	0.0	0.0

Table 2-6. Reduced lateral energy deposition of p, n, π^- induced showers at the sixth iron row.
 $(10^3/E_0)(\Delta E_{Fe6}/\Delta R)$ at 110cm depth of Fe/Ar sandwich.
 $(E_{cut}=100\text{MeV}, N=5000, \text{the 1-st interaction is forced on Fe1}).$

a) Proton induced showers.

$E_0, \text{ GeV}$	300	500	1000	2000	5000	10000	20000
1.	6.3 ± 0.6	8.3 ± 0.8	15.0 ± 1.5	17.0 ± 1.0	22.0 ± 2.0	28.0 ± 2.0	32.0 ± 2.0
2.	6.9 ± 0.8	7.2 ± 0.7	8.1 ± 0.8	10.0 ± 1.0	10.0 ± 1.0	11.0 ± 1.0	12.0 ± 1.0
4.	4.2 ± 0.4	5.0 ± 0.4	4.6 ± 0.4	5.8 ± 0.5	6.0 ± 0.5	5.2 ± 0.4	5.3 ± 0.5
6.	3.3 ± 0.3	3.0 ± 0.3	3.2 ± 0.3	3.5 ± 0.4	3.0 ± 0.3	3.0 ± 0.3	3.9 ± 0.4
8.	2.9 ± 0.2	2.4 ± 0.2	2.2 ± 0.2	2.3 ± 0.2	1.7 ± 0.2	1.8 ± 0.2	2.2 ± 0.3
10.	1.9 ± 0.2	1.4 ± 0.1	1.7 ± 0.2	1.5 ± 0.2	1.5 ± 0.2	1.4 ± 0.2	1.1 ± 0.2
20.	0.81 ± 0.05	0.87 ± 0.07	0.73 ± 0.06	0.9 ± 0.2	0.7 ± 0.06	0.59 ± 0.05	0.54 ± 0.05
40.	0.33 ± 0.1	0.18 ± 0.01	0.45 ± 0.03	0.22 ± 0.05	0.17 ± 0.03	0.1 ± 0.01	0.096 ± 0.01
80.	0.025 ± 0.003	0.018 ± 0.002	0.018 ± 0.002	0.019 ± 0.003	0.014 ± 0.003	0.008 ± 0.002	0.011 ± 0.003
150.	0.001 ± 0.0002	0.003 ± 0.001	0.0034 ± 0.001	0.004 ± 0.002	0.0004 ± 0.0001	0.0004 ± 0.0001	0.0005 ± 0.0001

2-6. b) Neutron induced showers.

E_0 , GeV	300	500	1000	2000	5000	10000	20000
1.	1.56 ± 0.6	1.7 ± 0.7	11.0 ± 1.0	117.0 ± 1.0	126.0 ± 2.0	124.0 ± 2.0	127.0 ± 2.0
2.	1.72 ± 0.7	1.6 ± 0.9	1.90 ± 0.9	110.0 ± 1.0	111.0 ± 1.0	110.0 ± 1.0	110.0 ± 1.0
4.	1.61 ± 1.0	1.48 ± 0.4	1.59 ± 0.6	1.46 ± 0.3	1.59 ± 0.6	1.46 ± 0.4	1.50 ± 0.4
6.	1.45 ± 1.0	1.25 ± 0.2	1.30 ± 0.3	1.33 ± 0.3	1.29 ± 0.3	1.34 ± 0.4	1.30 ± 0.3
8.	1.21 ± 0.2	1.24 ± 0.3	1.24 ± 0.2	1.19 ± 0.1	1.20 ± 0.3	1.19 ± 0.2	1.16 ± 0.2
10.	1.16 ± 0.1	1.17 ± 0.2	1.15 ± 0.1	1.15 ± 0.2	1.12 ± 0.2	1.08 ± 0.08	1.10 ± 0.1
20.	1.086 ± 0.1	1.079 ± 0.05	1.079 ± 0.06	1.072 ± 0.05	1.059 ± 0.05	1.058 ± 0.05	1.05 ± 0.06
40.	1.025 ± 0.04	1.02 ± 0.02	1.02 ± 0.02	1.014 ± 0.01	1.013 ± 0.01	1.0089 ± 0.01	1.0089 ± 0.009
80.	1.0035 ± 0.004	1.0026 ± 0.003	1.002 ± 0.003	1.0017 ± 0.002	1.0015 ± 0.002	1.0011 ± 0.003	1.001 ± 0.002
150.	1.0002 ± 0.0004	1.0001 ± 0.0001	1.0015 ± 0.0004	1.00008 ± 0.0003	1.0005 ± 0.0001	1.00003 ± 0.00008	1.00011 ± 0.0008

2-6. c) Pion induced showers.

$E_0, \text{ GeV}$	300	500	1000	2000	5000	10000	20000
$R, \text{ cm}$							
1.	6.4 ± 1.0	9.5 ± 1.0	11.0 ± 1.0	11.0 ± 1.0	12.0 ± 2.0	22.0 ± 2.0	22.0 ± 2.0
2.	6.1 ± 1.0	5.4 ± 0.6	8.1 ± 1.0	8.2 ± 1.0	9.0 ± 1.0	7.5 ± 0.9	9.2 ± 1.0
4.	3.5 ± 0.4	4.1 ± 0.5	4.5 ± 0.5	4.0 ± 0.5	5.1 ± 0.7	4.2 ± 0.5	4.4 ± 0.5
6.	2.3 ± 0.2	3.2 ± 0.7	2.7 ± 0.3	2.0 ± 0.2	2.4 ± 0.4	2.3 ± 0.3	1.6 ± 0.2
8.	1.9 ± 0.2	1.6 ± 0.2	1.6 ± 0.2	1.3 ± 0.2	1.5 ± 0.2	1.6 ± 0.3	1.4 ± 0.3
10.	1.7 ± 0.3	1.5 ± 0.2	1.5 ± 0.3	1.0 ± 0.2	0.79 ± 0.1	0.89 ± 0.2	0.83 ± 0.1
20.	0.58 ± 0.05	0.89 ± 0.1	0.79 ± 0.09	0.49 ± 0.06	0.47 ± 0.05	0.45 ± 0.06	0.38 ± 0.06
40.	0.14 ± 0.01	0.24 ± 0.04	0.26 ± 0.04	0.12 ± 0.01	0.12 ± 0.02	0.072 ± 0.01	0.085 ± 0.02
80.	0.032 ± 0.01	0.016 ± 0.003	0.022 ± 0.003	0.01 ± 0.002	0.007 ± 0.002	0.007 ± 0.003	0.004 ± 0.0009
150.	0.001 ± 0.0003	0.0034 ± 0.002	0.0035 ± 0.002	0.0003 ± 0.0001	0.0005 ± 0.0002	0.003 ± 0.001	0.0008 ± 0.0005

Table 2-7. Coefficients used in the parametrization of dE/dX (formula (2.1)), E_p is in GeV.

The primary is a proton	
$a = -0.5 (\pm 0.2) + 0.8 (\pm 0.1) \lg E_p$	
$b = 0.01 (\pm 0.002) \lg E_p$	
$c = 1.1 (\pm 0.1) \lg E_p$	
$d = 1.1 (\pm 0.1) + 0.35 (\pm 0.06) \lg E_p$	
$\lg W_1 = 0.6 (\pm 0.2) - 1.0 (\pm 0.08) \lg E_p$	
The primary is a neutron	
$a = -0.5 (\pm 0.2) + 0.75 (\pm 0.08) \lg E_p$	
$b = 0.01 (\pm 0.002) \lg E_p$	
$c = 1.3 (\pm 0.2) \lg E_p$	
$d = 0.7 (\pm 0.4) + 0.5 (\pm 0.1) \lg E_p$	
$\lg W_1 = 1.2 (\pm 0.3) - 1.1 (\pm 0.09) \lg E_p$	
The primary is a π -meson	
$a = -0.7 (\pm 0.3) + 0.9 (\pm 0.1) \lg E_p$	
$b = 0.01 (\pm 0.003) \lg E_p$	
$c = 1.4 (\pm 0.2) \lg E_p$	
$d = 1.8 (\pm 0.5) + 0.3 (\pm 0.1) \lg E_p$	
$\lg W_1 = 1.0 (\pm 0.4) - 1.4 (\pm 0.1) \lg E_p$	

Table 2-8. Coefficients used in the parametrization of X_{max} (formula (2.6)).

The primary	τ	$\Delta \tau$
p	6.0	± 0.2
n	6.0	± 0.2
π	6.1	± 0.2

Table 2-9. Coefficients used in the parametrization of shower lateral profiles at the shower maximum in iron absorber (formula (2.7) and Table 2-4).

a) The primary is a proton

E_p , GeV	300	500	1000	2000	5000	10000	20000
N_1	0.0040±0.0031	0.207±0.0041	0.19±0.0031	0.18±0.0031	0.18±0.004	0.181±0.0041	0.18±0.004
W_1	0.84 ±0.06	0.54 ±0.13	0.74±0.04	0.70±0.04	0.78±0.08	0.59 ±0.06	0.58±0.07
P_1	2.15 ±0.16	1.40 ±0.6	1.52±0.44	1.76 ±0.7	3.74±0.43	11.05 ±2.5	7.48±1.23
P_2	0.48 ±0.35	1.43 ±0.16	1.04±0.11	1.12±0.09	0.88±0.19	1.178 ±0.12	1.58±0.16
κ_2	1.016	1.119	1.1492	1.2744	0.756	0.956	1.07

b) The primary is a neutron.

E_p , GeV	300	500	1000	2000	5000	10000	20000
N_1	0.21 ±0.003	0.201±0.0031	0.19 ±0.0031	0.18 ±0.0041	0.18 ±0.0031	0.18 ±0.0041	0.18 ±0.004
W_1	0.67 ±0.13	0.70 ±0.10	0.61 ±0.08	0.72 ±0.04	0.74 ±0.07	0.79 ±0.07	0.67±0.1
P_1	2.76 ±0.4	1.337 ±0.42	1.592 ±0.92	1.677 ±0.6	4.12 ±0.41	4.52 ±0.49	6.27 ±1.1
P_2	1.02 ±0.16	1.05 ±0.14	1.137 ±0.16	1.129 ±0.1	0.96 ±0.15	0.97 ±0.19	1.46 ±0.28
κ_2	1.2617	1.185	1.1018	1.0464	1.2095	1.0499	1.055

c) The primary is a π -meson.

E_0 , GeV	300	500	1000	2000	5000	10000	20000
N_T	0.206 ± 0.004	0.208 ± 0.004	0.20 ± 0.004	0.18 ± 0.004	0.19 ± 0.004	0.18 ± 0.004	0.18 ± 0.004
W_T	10.60 ± 0.06	10.69 ± 0.05	10.57 ± 0.04	10.73 ± 0.17	10.52 ± 0.02	10.62 ± 0.11	10.51 ± 0.12
P_1	1.71 ± 0.73	1.62 ± 0.68	1.79 ± 1.70	1.39 ± 0.61	1.98 ± 0.63	1.97 ± 1.50	1.10 ± 3.2
P_2	1.27 ± 0.12	1.04 ± 0.12	1.55 ± 0.11	1.11 ± 0.32	1.54 ± 0.06	1.49 ± 0.26	1.94 ± 0.32
χ^2	1.552	1.059	1.709	1.061	1.004	1.0379	1.11

Table 2-10. Leakage from the "PID" calorimeter. The 1-st interaction is forced on PbI, number of showers is 5000, hadron cutoff energy is 100MeV.

a) The primary is a proton.

Incident Energy, TeV	Leakage Energy, GeV										
	Hadrons			Low-Energy Neutrons	Photons and Electrons	Total			Number of Leakage Particles		
	Backward	Forward	Side	Neutrons	Electrons	Backward	Forward	Side	Backward	Forward	Side
0.3	0.536	14.28	0.262	0.151	2.387	17.62	3.2	12.3	1.7		
0.5	0.418	23.32	0.157	0.2	3.734	27.83	2.6	20.7	0.8		
1.	0.479	59.41	0.573	0.273	11.31	72.04	2.9	45.	3.6		
2.	0.6	140.9	0.757	0.337	25.99	168.6	3.8	76.7	4.6		
5.	0.8	365.2	1.873	0.474	73.79	442.2	5.3	190.4	10.0		
10.	0.99	864.2	3.558	0.696	192.5	1062.	6.6	395.	19.8		
20.	1.532	1683.	6.318	0.602	428.3	1320.	10.5	704.	34.2		

2-10. b) The primary is a neutron.

Incident Energy, TeV	Leakage Energy, GeV										
	Hadrons			Low-Energy Neutrons	Photons and Electrons	Total			Number of Leakage Particles		
	Backward	Forward	Side	Neutrons	Electrons	Backward	Forward	Side	Backward	Forward	Side
0.3	0.384	13.64	0.223	0.169	2.338	16.75	2.5	14.3	1.2		
0.5	0.45	22.59	0.403	0.214	4.063	27.72	2.7	21.	2.1		
1.	0.715	62.33	0.493	0.28	9.468	73.29	5.3	44.9	2.3		
2.	0.481	139.7	1.071	0.361	27.83	169.4	3.1	90.4	5.3		
5.	0.677	400.	2.274	0.449	62.16	465.5	4.6	211.8	14.1		
10.	1.372	835.	3.233	0.581	178.9	1019.	9.6	396.4	17.4		
20.	1.21	1766.	3.314	0.719	443.1	1215.	7.7	701.7	17.4		

2-10. c) The primary is a pion.

Incident Energy, TeV	Leakage Energy, GeV						Number of Leakage Particles		
	Hadrons			Low-Energy	Photons	Total	Backward	Forward	Side
	Backward	Forward	Side	Neutrons	and Electrons				
0.3	0.241	9.621	0.143	0.125	1.851	11.98	1.7	9.7	0.8
0.5	0.223	21.4	0.492	0.138	3.621	25.87	1.6	13.7	3.9
1.	0.318	39.3	0.355	0.14	7.151	47.31	2.1	30.9	2.
2.	0.331	82.3	0.349	0.177	15.59	98.74	2.1	51.8	2.1
5.	0.394	320.	0.905	0.256	50.84	372.4	2.5	136.8	5.8
10.	0.53	666.	0.84	0.335	160.3	827.9	3.4	249.9	4.4
20.	0.69	1240.	1.808	0.291	318.6	1561.	4.9	387.6	10.6

Table 2-11. Leakage from the "PION" calorimeter. The 1-st interaction is anywhere in Pb/Ar/Fe, number of showers is 5000, hadron cutoff energy is 100MeV.

a) The primary is a proton.

Incident Energy, TeV	Leakage Energy, GeV						Number of Leakage Particles		
	Hadrons			Low-Energy	Photons	Total	Backward	Forward	Side
	Backward	Forward	Side	Neutrons	and Electrons				
0.3	0.051	25.52	0.288	0.029	3.062	28.99	0.6	18.5	1.7
0.5	0.053	45.84	0.425	0.031	7.232	53.58	0.3	32.2	2.7
1.	0.106	112.1	0.38	0.041	19.76	132.3	0.8	64.6	2.
2.	0.17	240.7	0.744	0.042	50.54	292.2	1.2	121.8	4.
5.	0.245	647.5	1.605	0.034	144.9	794.3	1.7	221.7	9.6
10.	0.226	1367.	2.571	0.051	371.	1741.	1.5	448.4	13.9
20.	0.344	2692.	1.573	0.098	817.	3511.	2.4	728.9	7.9

2-11. b) The primary is a neutron.

Incident Energy, TeV	Leakage Energy, GeV						Number of Leakage Particles		
	Hadrons			Low-Energy	Photons	Total	Backward	Forward	Side
	Backward	Forward	Side	Neutrons	and Electrons				
0.3	0.057	27.51	0.177	0.022	3.87	31.63	0.4	17.9	1.
0.5	0.058	46.5	0.163	0.036	7.07	53.83	0.4	29.	0.8
1.	0.087	104.6	0.278	0.038	19.41	124.4	0.6	55.4	1.5
2.	0.094	232.2	1.256	0.028	5.03	278.6	0.6	114.6	7.3
5.	0.123	648.7	0.662	0.033	153.5	803.	0.9	216.3	3.6
10.	0.244	1392.	1.153	0.114	350.6	1744.	1.7	456.7	6.9
20.	0.195	2784.	2.74	0.073	748.7	3536.	1.4	712.7	14.

2-11. c) The primary is a pion.

Incident Energy, TeV	Leakage Energy, GeV						Number of Leakage Particles		
	Hadrons			Low-Energy Neutrons	Photons and Electrons	Total	Backward	Forward	Side
	Backward	Forward	Side						
0.3	0.02	24.26	0.075	0.021	4.073	28.45	0.1	15.8	0.4
0.5	0.037	46.88	0.102	0.021	7.189	54.22	0.2	24.6	0.6
1.	0.062	89.41	0.214	0.022	18.92	108.6	0.4	40.3	1.4
2.	0.053	210.3	0.332	0.026	49.82	260.6	0.4	108.7	2.
5.	0.046	567.6	0.577	0.037	156.5	724.7	0.3	211.8	3.4
10.	0.091	931.7	1.863	0.033	266.4	1200.	0.7	284.7	10.9
20.	0.1	2107.	1.454	0.081	583.2	12692.	0.7	417.5	10.3

Table 2-12 Leakage from the "PION" calorimeter. The 1-st interaction is on Fe, number of showers is 5000, hadron cutoff energy is 100MeV.

a) The primary is a proton.

Incident Energy, TeV	Leakage Energy, GeV						Number of Leakage Particles		
	Hadrons			Low-Energy Neutrons	Photons and Electrons	Total	Backward	Forward	Side
	Backward	Forward	Side						
0.3	0.268	15.19	0.202	0.092	2.129	18.88	1.7	17.4	1.
0.5	0.31	30.45	0.265	0.127	5.401	36.55	1.9	23.5	1.6
1.	0.477	66.74	0.625	0.135	10.24	78.22	2.6	49.5	3.2
2.	0.41	151.9	0.793	0.177	28.34	181.6	2.7	92.9	4.4
5.	0.516	438.3	1.544	0.228	98.74	539.3	3.3	211.	8.1
10.	1.197	945.8	1.963	0.339	207.3	1157.	7.6	383.	11.5
20.	0.792	12085.	2.745	0.312	548.9	12638.	5.4	715.	17.9

2-12. b) The primary is a neutron.

Incident Energy, TeV	Leakage Energy, GeV						Number of Leakage Particles		
	Hadrons			Low-Energy Neutrons	Photons and Electrons	Total	Backward	Forward	Side
	Backward	Forward	Side						
0.3	0.242	14.18	0.221	0.102	2.049	16.8	1.5	15.	1.2
0.5	0.266	26.99	0.163	0.104	3.487	31.01	1.6	20.1	1.
1.	0.266	68.52	0.353	0.138	12.74	82.01	1.6	52.6	2.2
2.	0.477	161.1	0.506	0.189	29.19	191.5	3.2	84.7	3.1
5.	0.551	480.4	2.689	0.26	102.3	586.2	3.6	199.1	17.8
10.	0.557	11027.	2.554	0.262	195.8	11226.	3.9	418.8	14.2
20.	1.096	11860.	2.669	0.343	460.6	12325.	8.1	610.4	12.1

2-12. c) The primary is a pion.

Incident Energy, TeV	Leakage			Energy, GeV			Number of Leakage Particles		
	Backward	Forward	Side	Low-Energy Neutrons	Photons and Electrons	Total	Backward	Forward	Side
0.3	0.127	12.04	0.198	0.063	1.87	14.29	0.8	10.2	0.9
0.5	0.175	23.09	0.141	0.069	3.358	26.83	1.2	18.6	1.
1.	0.197	56.92	0.311	0.098	9.325	66.85	1.4	37.3	1.8
2.	0.167	114.	0.307	0.113	21.88	136.5	1.1	62.	1.9
5.	0.288	371.4	0.688	0.147	79.71	452.2	1.8	183.6	4.1
10.	0.308	718.4	1.092	0.218	142.8	862.8	2.1	256.5	6.2
20.	0.278	1684.	2.165	0.243	402.9	2089.	2.1	458.8	11.7

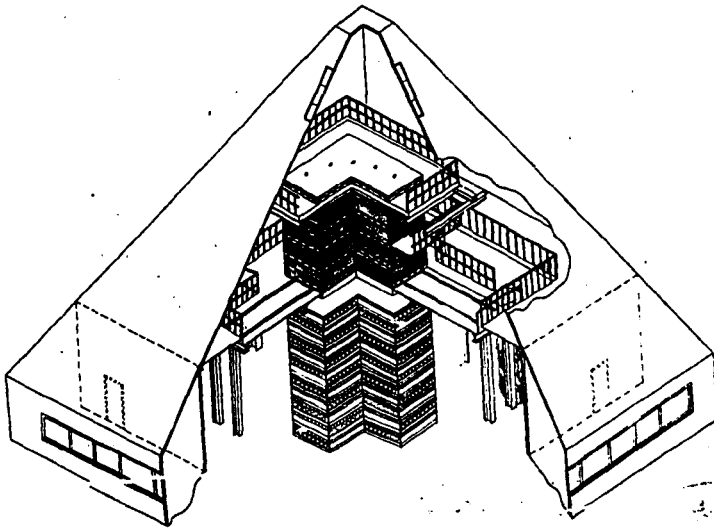


Fig. 2.1

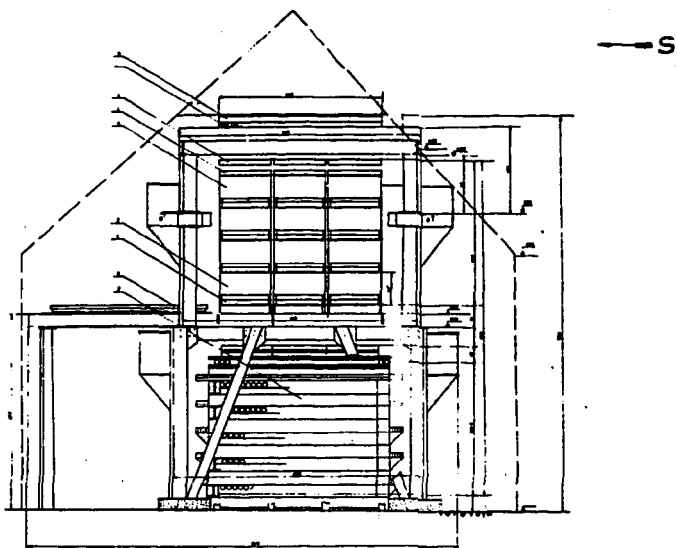


Fig. 2.2

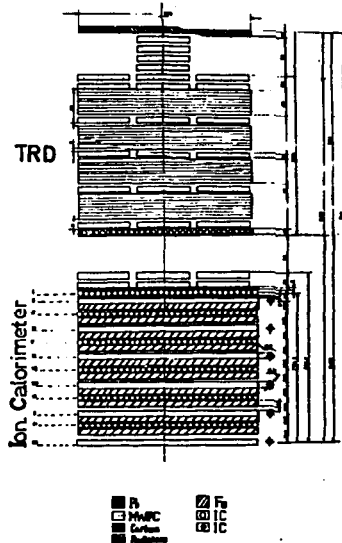


Fig. 2.3

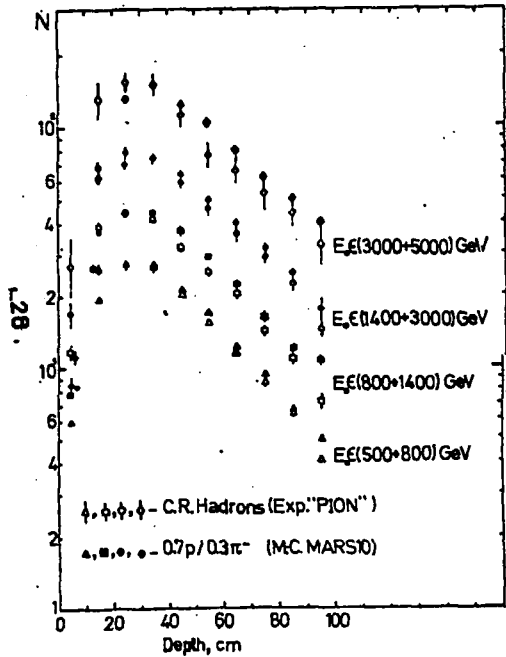


Fig. 2.4

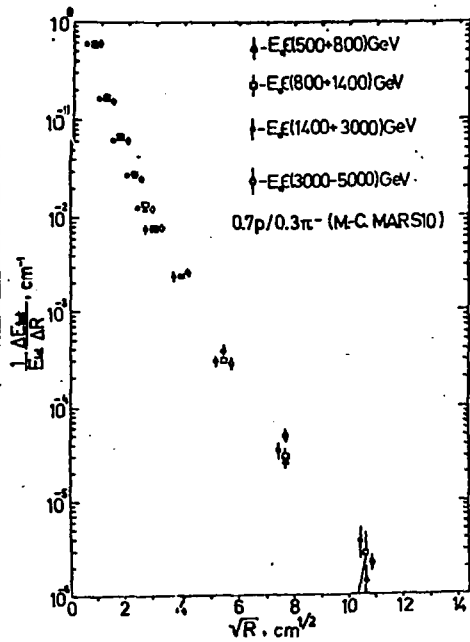


Fig. 2.5

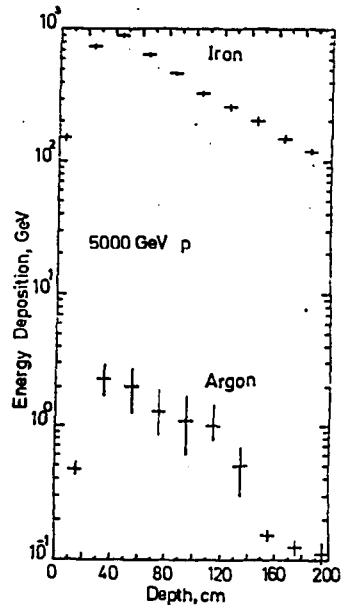


Fig. 2.6

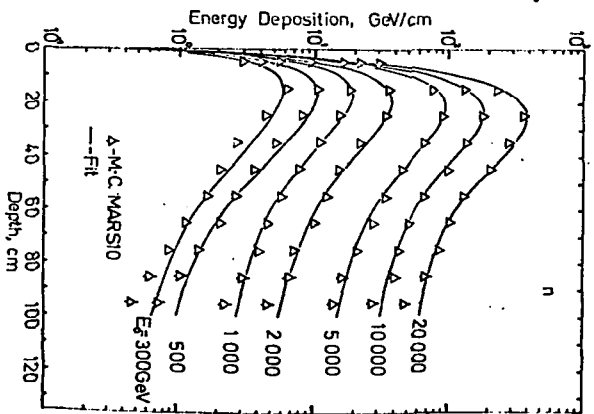
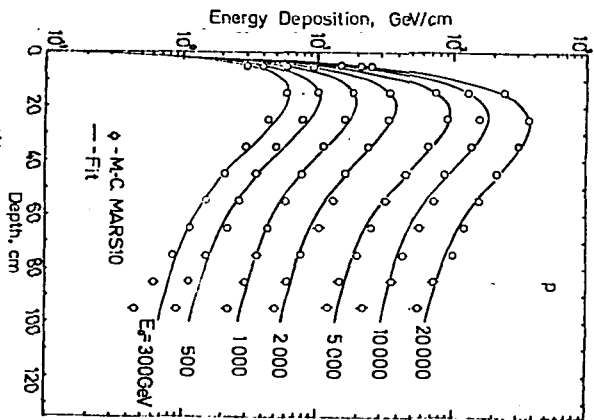


Fig. 2.8

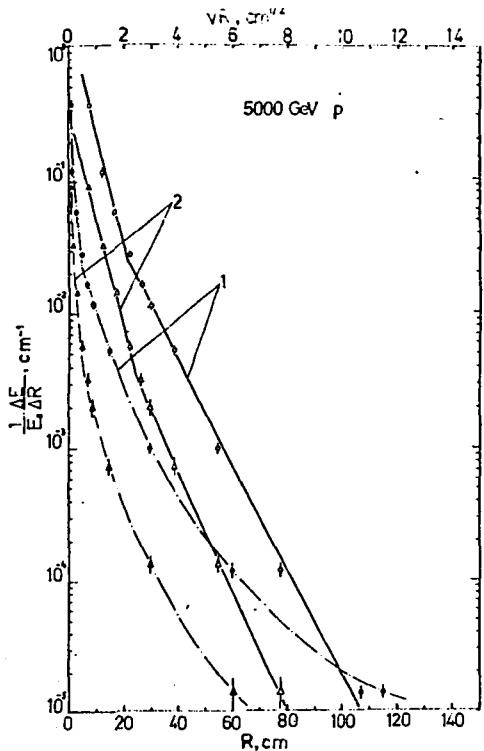


Fig. 2.7

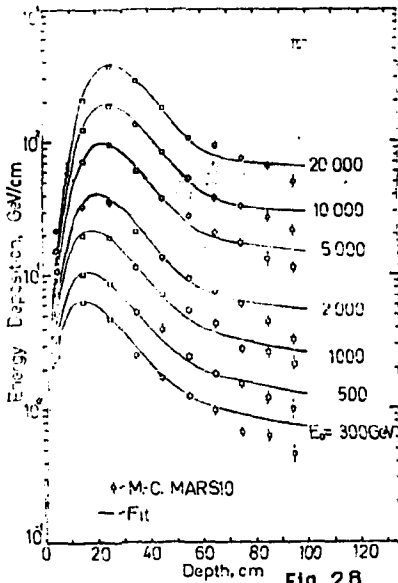


Fig. 2.8

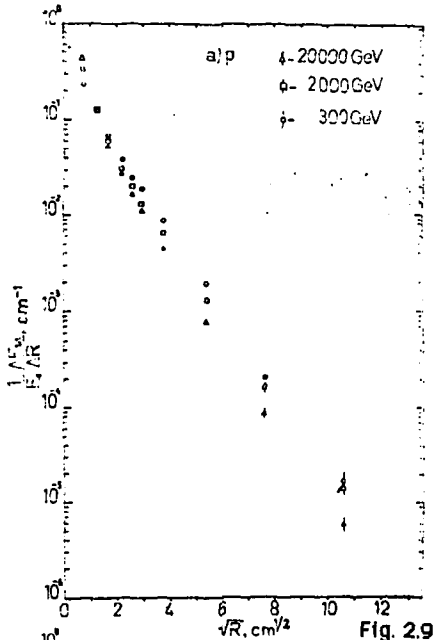


Fig. 2.9

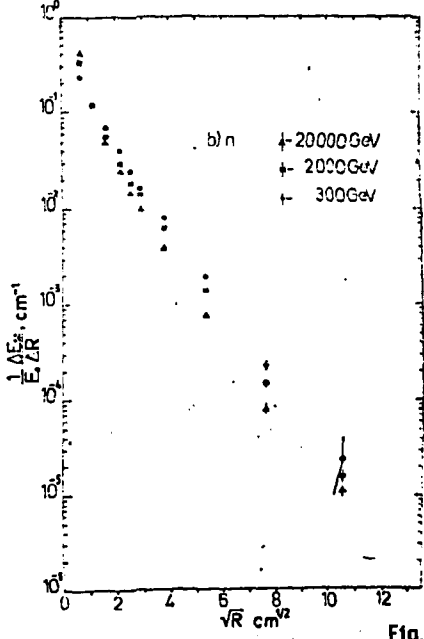
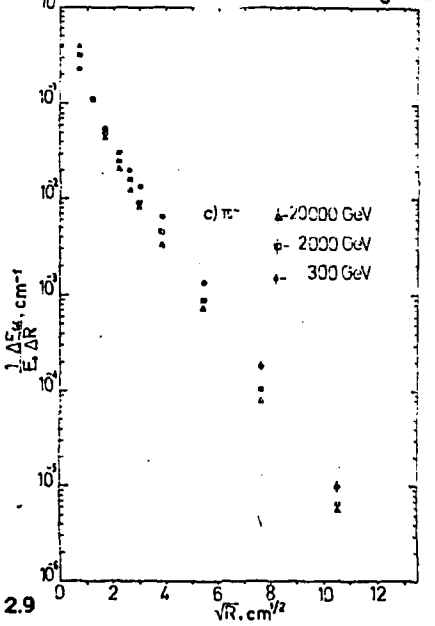


Fig. 2.9



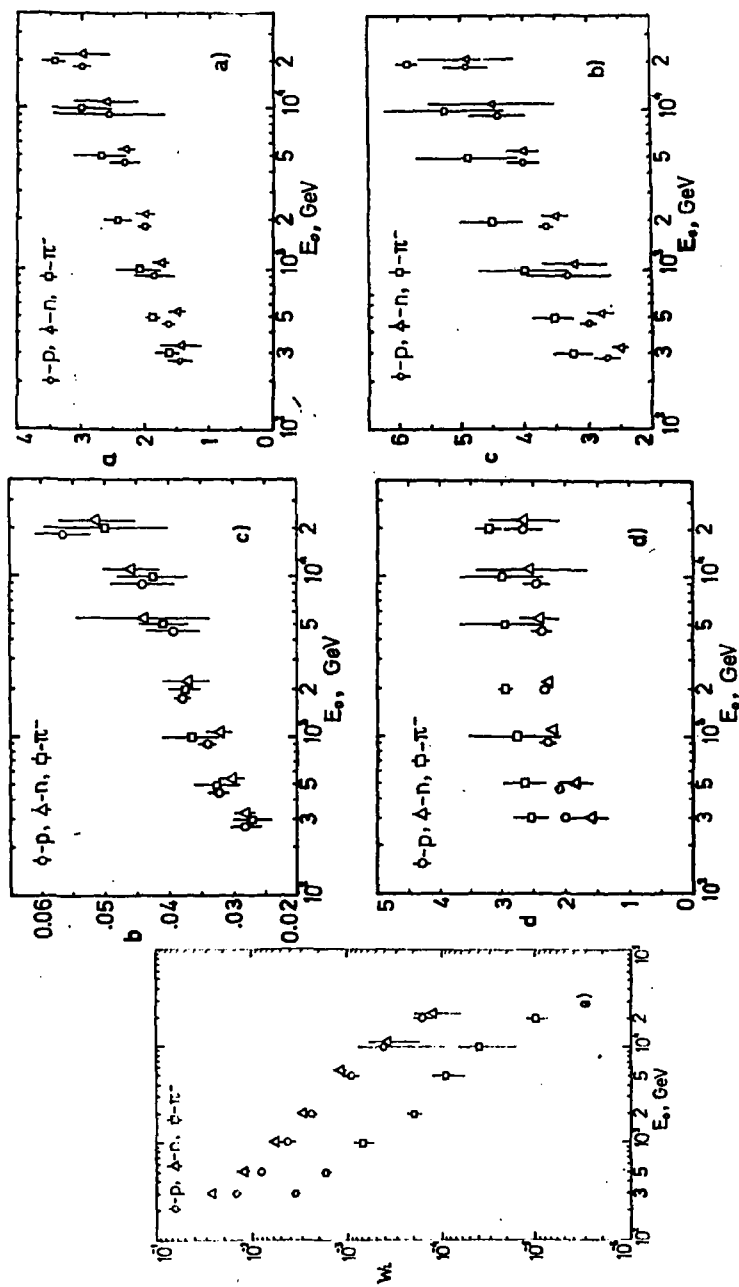


Fig. 2.10

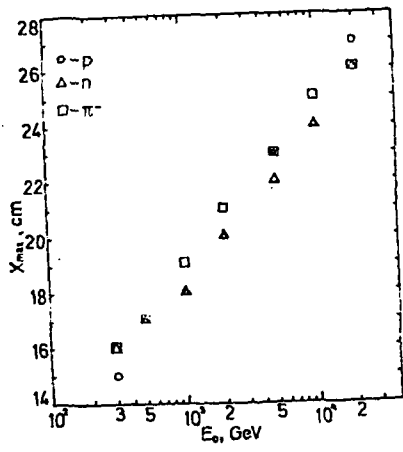


Fig. 2.11

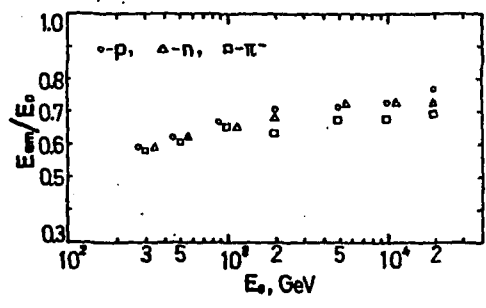


Fig. 2.12

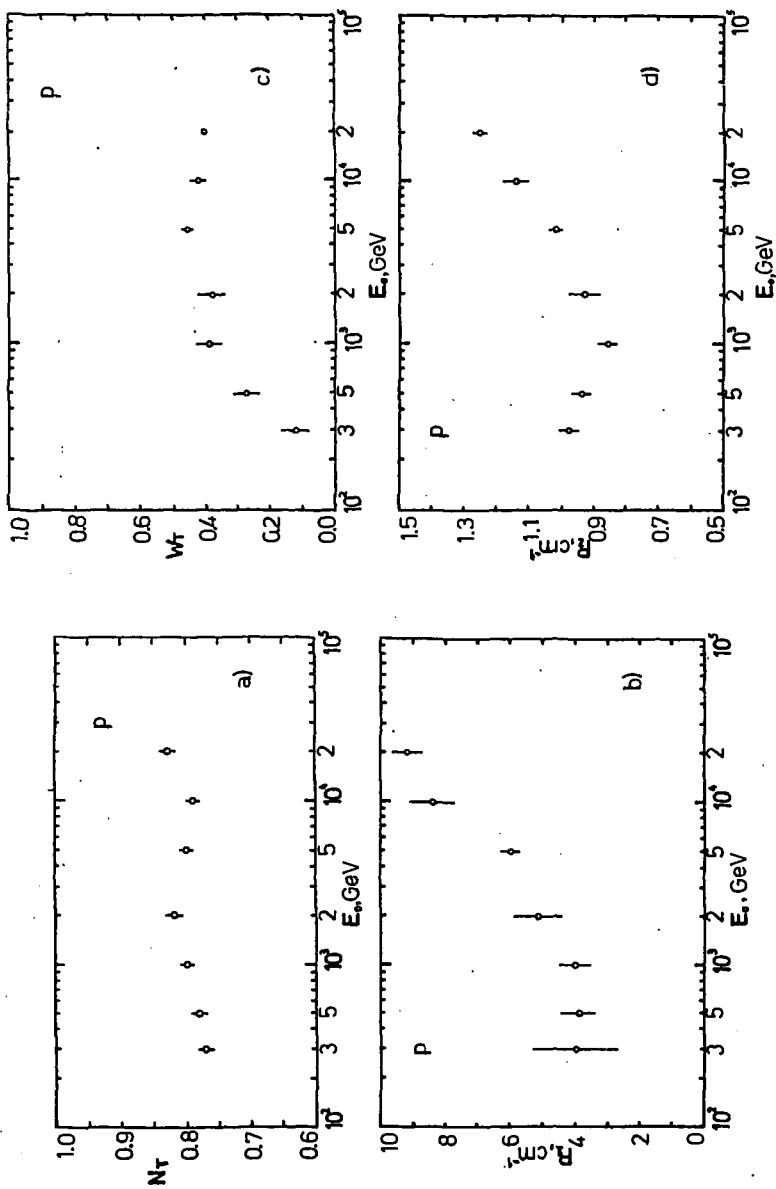


Fig. 2.13

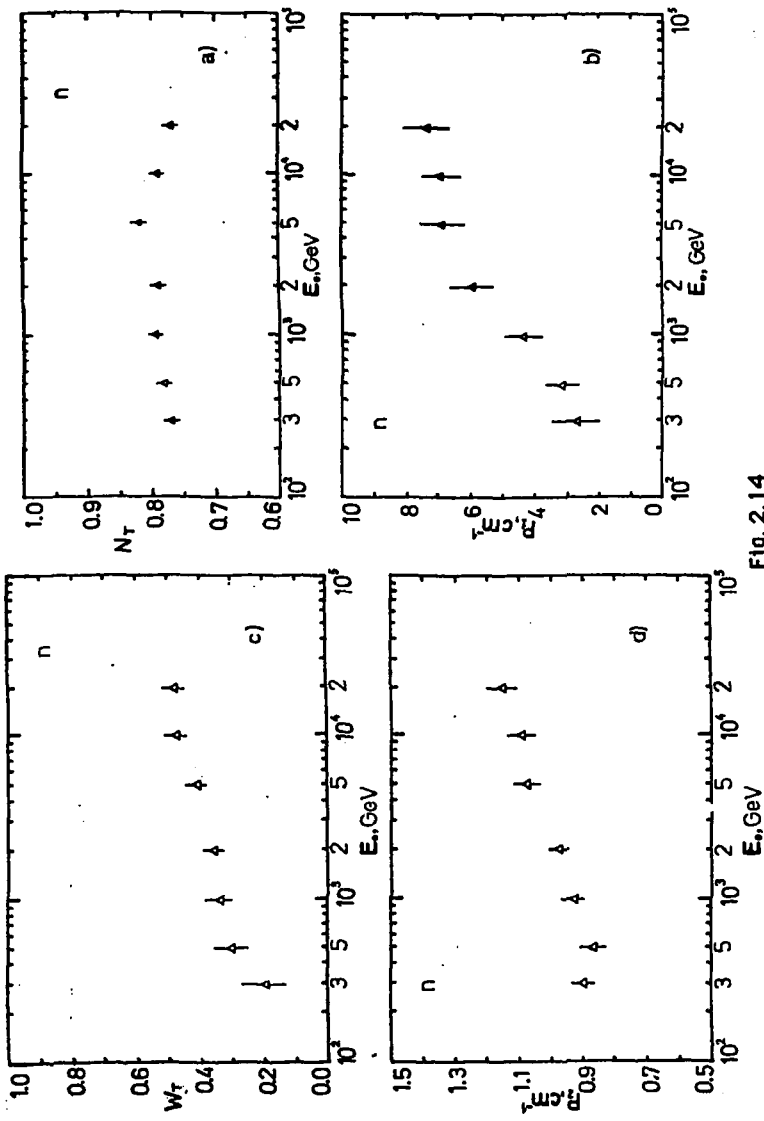


Fig. 2.14

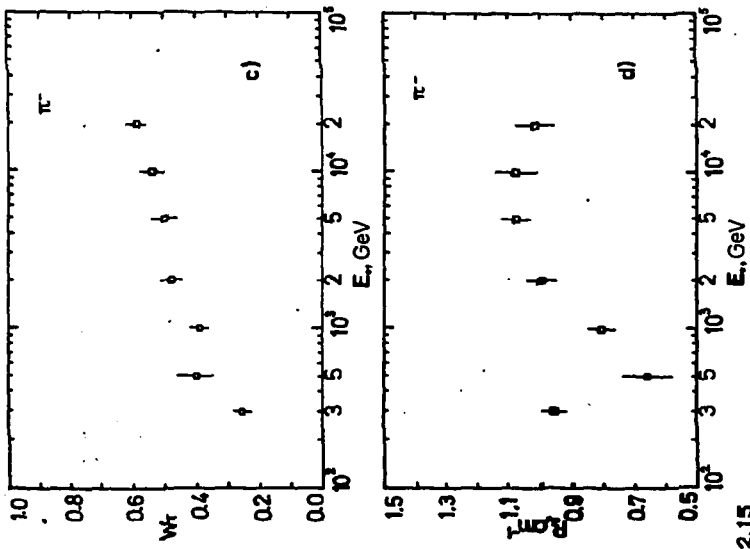


Fig. 2.15

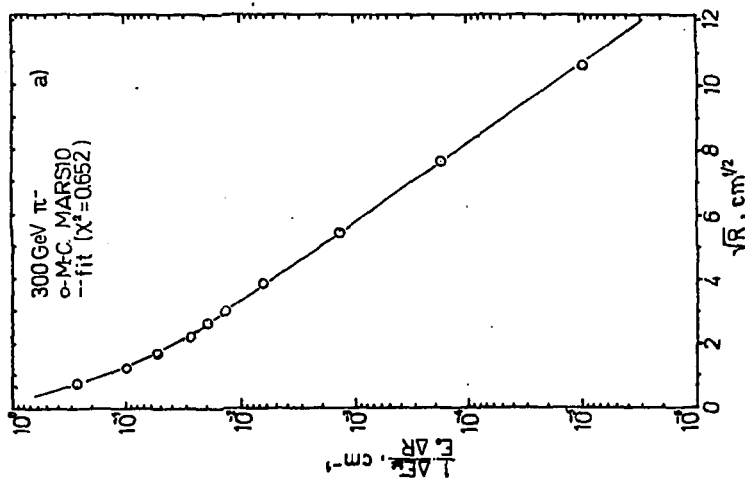
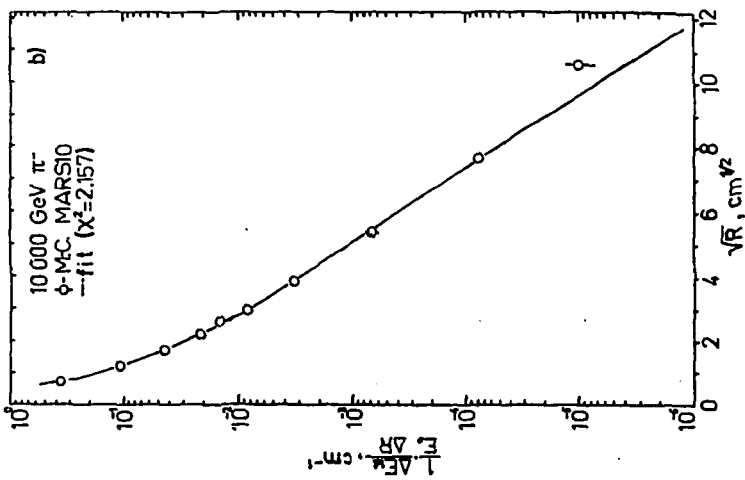


Fig. 2.1

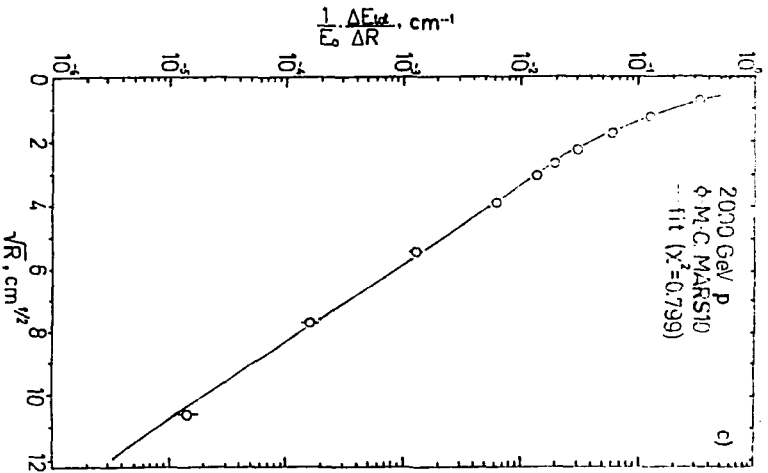


Fig. 2.16

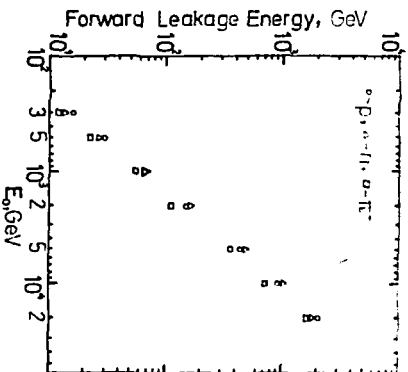


Fig. 2.17

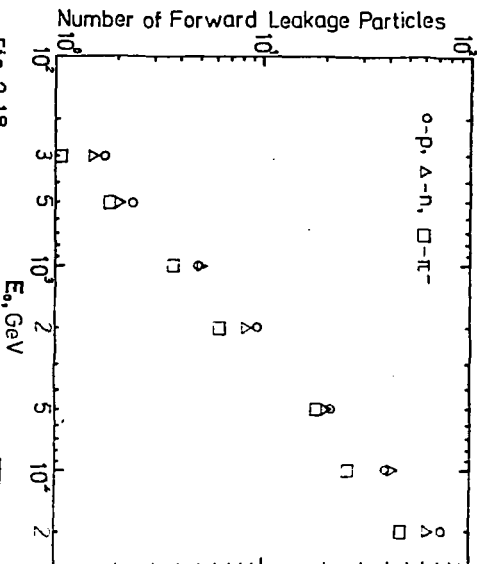


Fig. 2.18

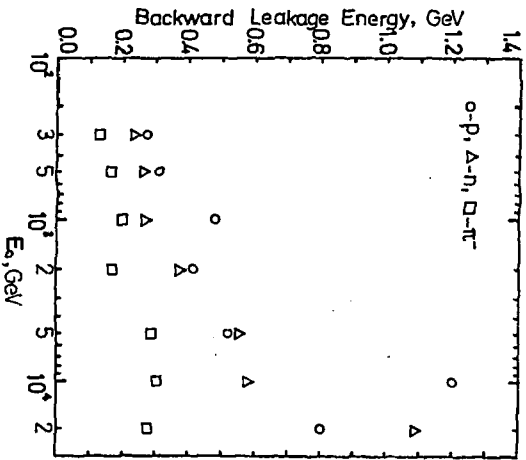


Fig. 2.19

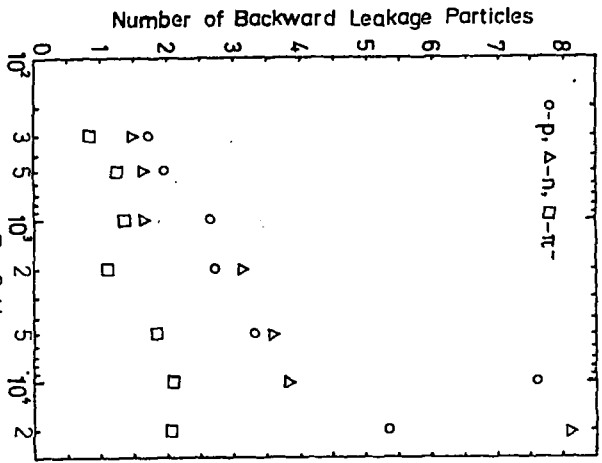


Fig. 2.20

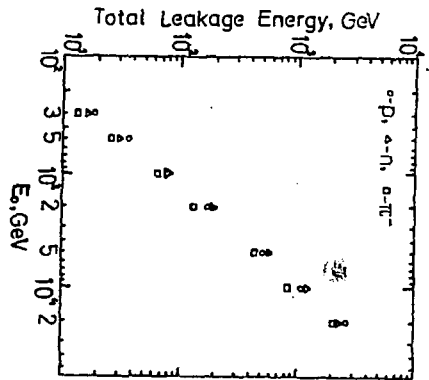


Fig. 2.21

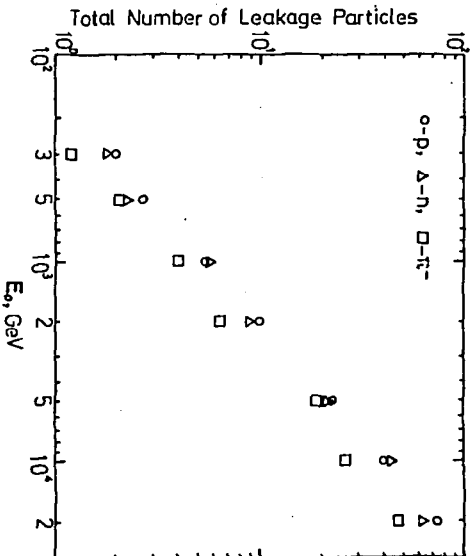


Fig. 2.22

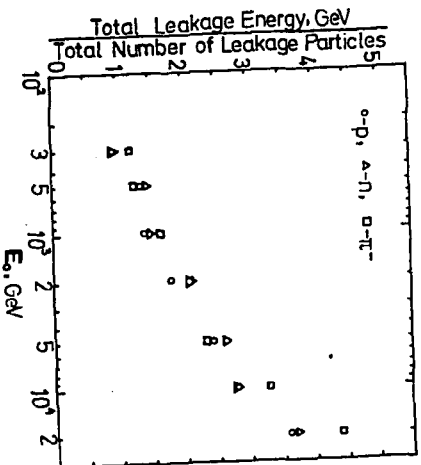


Fig. 2.23

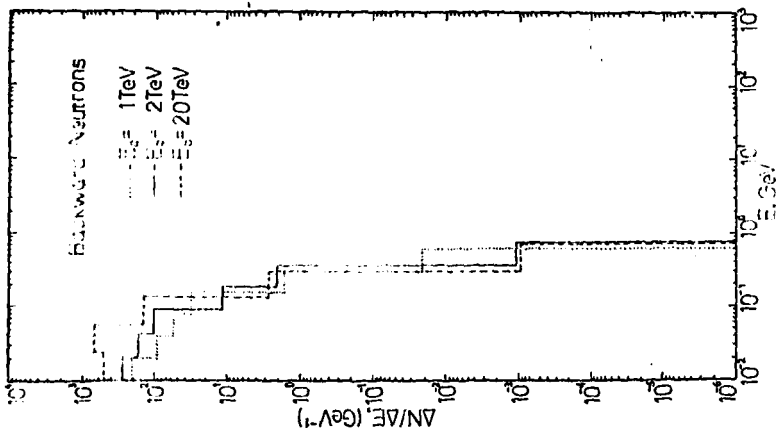


Fig. 2.25

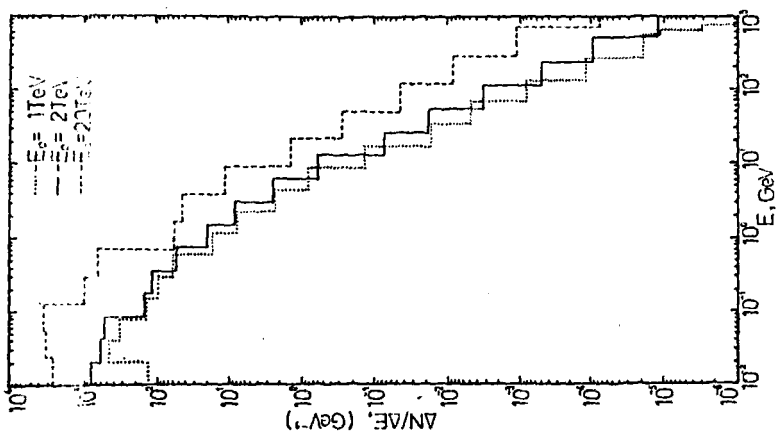


Fig. 2.24

FIGURE CAPTIONS

Fig. 2.1. Artists view of the "PION" setup.

Fig. 2.2. Schematic drawing of the "PION" setup (the dimensions are in cm).

Fig. 2.3. Schematic layout of the PION setup showing the location of elements (the dimensions are in cm).

Fig. 2.4. Dependence of the total laterally integrated energy deposition on depth in iron absorber.

Fig. 2.5. Reduced lateral shower profiles.

Fig. 2.5. The average longitudinal shower profile in the PION calorimeter. The primary is a 5000GeV proton, the cutoff energy is 100MeV, the number of shower histories is 5000.

Fig. 2.7. Longitudinally integrated lateral shower profiles: ϕ - lower scale, ψ - upper scale. Lateral shower profile at the shower maximum: \uparrow - lower scale, \downarrow - upper scale. The primary is 5000GeV proton.

Fig. 2.8. Longitudinal shower profiles for proton a), neutron -b) and pion - c) initiated showers.

Fig. 2.9. Longitudinally integrated lateral profiles for proton - a), neutron - b) and pion - c) initiated showers.

Fig. 2.10. Dependence of the shape parameters of eq. (2.1) on primary energy for proton - ϕ , neutron - ψ and pion - χ initiated showers.

Fig. 2.11. Dependence of shower maximum depth on incident energy for proton (o), neutron (Δ) and pion (\square) induced showers. The shower depth is evaluated from the first interaction point.

Fig. 2.12. The fraction of electromagnetic energy deposition as a function of primary energy. The overlapping points are displaced horizontally.

Fig. 2.13. Dependence of the shower lateral profile parameters from eq. (2.7) on primary energy for proton induced showers.

Fig. 2.14. The same as in fig. 2.13 for neutron induced showers.

Fig. 2.15. The same as in fig. 2.14 for pion induced showers.

Fig. 2.16. Longitudinally integrated lateral shower profiles: a) - 300GeV pions, b) - 10TeV pions, c) - 2TeV protons.

Fig. 2.17. Dependence of the leakage energy for proton, neutron and pion induced showers on primary energy (see also Table 2.12).

Fig. 2.18. Dependence of the average number of leakage particles on primary energy for proton, neutron and pion induced showers (see also Table 2.12).

Fig. 2.19. Dependence of the total average energy carried by albedo particles for proton, neutron and pion induced showers on incident energy.

Fig. 2.20. Dependence of the average number of albedo particles on incident energy for proton neutron and pion induced showers (see also Table 2.12).

Fig. 2.21. Dependence of the total leakage energy on incident energy for proton, neutron and pion induced showers(see also Table 2.12).

Fig. 2.22. Dependence of the total number of leakage particles on incident energy for proton, neutron and pion induced showers (see also Table 2.12).

Fig. 2.23. Dependence of the average energy carried by one leakage particle on incident energy for proton, neutron and pion induced showers.

Fig. 2.24. The energy spectrum of leakage particles (protons, neutrons and charged pions). The primary is a proton, the first interaction is forced on Fe1, cutoff - 10MeV, $N=5000$, - $E_0 = 1\text{TeV}$, the total number of leakage particles is: 11.5 protons, 50.2 neutrons, 31.7 pions; ——— - $E_0 = 2\text{TeV}$, the total number of leakage particles is: 12.8 protons, 82.2 neutrons, 48.6 pions; - - - - $E_0 = 20\text{TeV}$, the total number of leakage particle is: 213 protons, 564 neutrons, 410 pions.

Fig. 2.25. The energy spectrum of albedo neutrons. The primary is a proton, the first interaction is forced on Fe1, cutoff - 10MeV, $N=5000$, - $E_0 = 1\text{TeV}$, 8.96 albedo neutrons; ——— - $E_0 = 2\text{TeV}$, 12.8 neutrons; - - - - $E_0 = 20\text{TeV}$, 40.3 neutrons.

REFERENCES

- [1] V. Avakyan et al., Preprint YPI-100(74), Yerevan, 1974.
- [2] V. Avakyan et al., Voprosi Atomnoy Nauki i Tekhniki, Seriya: Tekhnika Physicheskogo Experimentsa, 4(16), 3 (1983) (in Russian).
- [3] V. Avakyan et al., Proc. of the 2-nd International Symposium of Transition Radiation of High Energy Particles, 496-511, Yerevan, 1984.
- [4] V. Avakyan, Thesis, Yerevan Physics Institute, 1990.
- [5] V. Avakyan et al., Proc. of the 18-th ICRC, Bangalore, India, 1983, v.5, p. 263-266.
- [6] A. Havoundjyan, Thesis, Yerevan Physics Institute, 1983.
- [7] V. Avakyan et al., Yad. Phys., 41, 1163 (1985).
- [8] V. Avakyan et al., Nucl. Phys., B259, 163 (1985).
- [9] V. Avakyan et al., Yad. Phys., 50, 1348 (1989).
- [10] V. Avakyan et al., Proc. of the 21-st ICRC, HE 1.3-33, Adelaide, Australia, 145-148 (1990).
- [11] G. Gharegyozyan, Thesis, Yerevan Physics Institute, 1990.
- [12] V. Avakyan et al., Proc. of the 19-th ICRC, La Jolla, 6, 64, 1985.
- [13] V. Avakyan et al., Yad. Phys., 44, 1224 (1986).
- [14] V. Avakyan et al., Yad. Phys., 50, 705 (1989).
- [15] V. Avakyan et al., Proc. of the 21-st ICRC, Adelaide,

Australia, HE Sessions, v.8, 149-152 (1990).

[16] H. Ohanyan, Thesis, Yerevan Physics Institute, 1990.

[17] V. Avakyan et al., Nucl. Phys., **8259**, 156 (1985).

[18] M. Mouradyan and S. Sokhoyan, Preprint YPI-1302(88)-90, Yerevan, 1990 (in Russian).

[19] V. Avakyan et al., Yad. Phys., **54(6)** (1991).

[20] S. Sokhoyan, Thesis, Yerevan Physics Institute, 1991.

[21] G. Hovsepyan, Thesis, Yerevan Physics Institute, 1990.

[22] A. Kalinovski, N. Mokhov and Yu. Nikitin, Passage of High Energy Particles Through Matter, Energoatomizdat, Moscow, 1985 (in Russian).

[23] N. Mokhov and J. Cassairt, Fermilab Report, FN-424 (1985).

[24] Ts. Amatuni, E. Memidjanyan and Kh. Senossyan, Part I of this work, Preprint YPI-1381(11)-92, Yerevan, 1992.

[25] V. Avakyan et al., Preprint YPI-995(45)-87, Yerevan, 1987 (in Russian).

[26] R. Bock et al., NIM, **186**, 533 (1981).

[27] W. Womersley et al., Preprint Fermilab, FNAL-Pub-87/159 (1987).

[28] M. Abramowitz and I. Stegun, Handbook of Mathematical Functions, NBS Applied Mathematics, Series-55, 1964.

[29] CERN Program Library.

The manuscript was received 28th Febr. 1991.

Ц. А. АМАТУНИ, Э. А. МАМИДЖАНЫН, Х. Н. САНОСЯН

МОДЕЛИРОВАНИЕ АДРОННЫХ ЛИВНЕЙ МЕТОДОМ МОНТЕ-КАРЛО
ЧАСТЬ 2: КАЛОРИМЕТР УСТАНОВКИ "ПИОН"

(на английском языке)

Редактор А.С.Есин

Технический редактор А.С.Абрамян

Подписано в печать 5/ХП-92г.

Формат 60x84x16

Оффсетная печать. Уч.изд.л. 3,8

Тираж 100 экз. Ц.30 р.

Зак.тип. 063

Индекс 3649

Отпечатано в Ереванском физическом институте

Ереван-36, ул.Братъев аликханын,2

The address for requests:
Information Department
Yerevan Physics Institute
Alikhanian Brothers 2,
Yerevan, 375036
Armenia,

ИНДЕКС 3649



ЕРЕВАНСКИЙ ФИЗИЧЕСКИЙ ИНСТИТУТ